

Small polaron transport and pressure dependence of the electrical resistivity of $\text{La}_{2-x}\text{Sr}_x\text{NiO}_4$ ($0 \leq x \leq 1.2$)

Guoqing Wu* and J. J. Neumeier†

Department of Physics, Florida Atlantic University, Boca Raton, Florida 33431

(Received 9 August 2002; revised manuscript received 31 December 2002; published 19 March 2003)

Measurements of the electrical resistivity ρ as a function of temperature T and pressure P ($P \leq 1.6$ GPa) are reported on $\text{La}_{2-x}\text{Sr}_x\text{NiO}_4$ ($0 \leq x \leq 1.2$). A compositionally induced M - I transition occurs for $x \geq 0.9$. The data suggest small dielectric polaron conduction, with thermal-activated behavior at high temperatures and with three-dimensional variable range hopping at low temperatures for all compositions. Pressure is shown to weakly affect ρ , for example, near room temperature a rate of $-8.2\%/ \text{GPa}$ ($d\rho/dP = -0.57 \text{ m}\Omega/\text{GPa}$) is observed for $x = 0.8$. Fits to the data for the same composition in the temperature range $100 \text{ K} \leq T \leq 300 \text{ K}$ provide a thermally activated polaron hopping energy $E_A = 30.3 \text{ meV}$ and $dE_A/dP = -2.80 \text{ (meV/GPa)}$. No superconductivity was observed at pressures up to 1.6 GPa and temperatures down to 4.2 K for any of the studied compositions. Our measurements provide strong evidence for polaron-dominated electrical conduction in these charge transfer gap materials.

DOI: 10.1103/PhysRevB.67.125116

PACS number(s): 62.50.+p, 71.38.-k, 72.80.-r, 71.30.+h

I. INTRODUCTION

The compound $\text{La}_{2-x}\text{Sr}_x\text{NiO}_4$ has been the subject of considerable attention due to its close relationship with the isostructural superconducting compound $\text{La}_{2-x}\text{Sr}_x\text{CuO}_4$.¹⁻⁵ Interest was further stimulated in 1989 by the observation of small magnetic and resistance anomalies at low temperatures in some nickel oxide samples⁶⁻⁸ which were thought to indicate the occurrence of superconductivity; these observations were not substantiated in later experiments.³ Charge and spin ordering has been observed in $\text{La}_{2-x}\text{Sr}_x\text{NiO}_4$ ($x \leq 0.5$) whereby doped holes segregate to form hole-rich domain walls separating domains of antiferromagnetically ordered spins (typical values $x = 0.20, 0.25, 0.33$, and 0.5);⁹⁻¹² neutron diffraction has shown that local charge order (or polaron ordering) occurs above the spin ordering temperature where the stripe phase forms.¹¹ Similar effects are observed in $\text{La}_2\text{NiO}_{4+\delta}$ with $\delta < 0.15$.¹³⁻¹⁵ Both La_2NiO_4 and La_2CuO_4 are strongly correlated 2D charge-transfer (CT) gap antiferromagnetic (AFM) insulators with electronic properties determined largely through transition metal ($3d$ orbital) and oxygen ($2p$ orbital) hybridization. Near the Fermi energy, narrow hybridized conduction bands with two dimensional character exist. Doping of holes leads to metallic behavior in the two systems and superconductivity in the cuprate; no superconductivity has yet been observed in the nickelate. A larger charge-transfer gap¹⁶ has been reported for the nickelate and it has been suggested that this system differs from the cuprate through stronger electron-phonon (e -ph) coupling, smaller charge carrier mobility,^{17,18} and larger magnetic localization¹⁹ which lead to an unusual competition among magnetic and charge degrees of freedom. The lack of superconductivity in $\text{La}_{2-x}\text{Sr}_x\text{NiO}_4$ for any x value could be due to the weaker metal-oxygen bond hybridization which results in a larger charge transfer gap.^{3,20}

Pressure is a fundamental thermodynamic variable which facilitates a controlled volume change of a physical system. It is an outstanding tool in the study of transition metal ox-

ides (TMO's) which have significant sensitivity to pressure. For example, the three-dimensional (3D) nickel oxide $R\text{NiO}_3$ ($R = \text{Pr}, \text{Nd}, \text{and Sm}$) exhibits an extraordinary pressure dependence of the metal-insulator (M - I) transition which is thought to occur as a result of the decrease of the CT gap as well as an increase in conduction bandwidth W ; its M - I transition temperature T_{MI} is depressed by pressure at a rate as large as $dT_{MI}/dP = -95 \text{ K/GPa}$.^{21,22} Sizable pressure effects are also observed in the ferromagnet $\text{La}_{1-x}\text{Ca}_x\text{MnO}_3$ ($0.2 < x < 0.45$).²³ Most recently, we have reported pressure effects on Ruddlesden-Popper (RP) phases $\text{La}_{n+1}\text{Ni}_n\text{O}_{3n+1}$ ($n = 2$ and 3).²⁴ We found that pressure drives T_{MI} of $\text{La}_3\text{Ni}_2\text{O}_7$ and $\text{La}_4\text{Ni}_3\text{O}_{10}$ to lower temperatures at modest rates of 11 and 7 K/GPa ,²⁴ respectively, and high pressures could completely depress their weak MI transitions. In general, pressure is expected to increase the metal-oxygen bond hybridization, thus decrease the CT gap. This could also lead to superconductivity or metal-insulator transitions as confirmed by the recent discoveries of superconductivity in sulfur²⁵ and oxygen.²⁶

In this report, the electrical resistivity of $\text{La}_{2-x}\text{Sr}_x\text{NiO}_4$ under hydrostatic pressure up to 1.6 GPa is investigated over a wide range of x ($0 \leq x \leq 1.2$). To our knowledge, the only high pressure measurements of the electrical resistivity of $\text{La}_{2-x}\text{Sr}_x\text{NiO}_4$ were reported for the charge ordering composition $x = 0.33$.²⁷ The charge ordering transition temperature T_{CO} of $\text{La}_{1.67}\text{Sr}_{0.33}\text{NiO}_4$ was observed to be weakly dependent on pressure. Most strikingly, no pressure measurements of the electrical resistivity have been conducted on $\text{La}_{2-x}\text{Sr}_x\text{NiO}_4$ in the important region where metallic behavior is observed ($0.8 \leq x \leq 1.2$). In this region, the localized magnetic moments on the Ni site are most negligible and the possibility for a superconducting ground state is high. It is suggested that the M - I transition is related to the ground state properties of highly correlated electron systems^{28,29} as that found in high temperature superconductors where the superconducting ground state occurs at doping levels where insulating behavior is suppressed³⁰ (e.g., $\text{La}_{2-x}\text{Sr}_x\text{CuO}_4$ is

metallic for $x > 0.05$ and shows superconductivity in the range $0.05 \leq x \leq 0.2$.³¹ In addition to this insulating-to-metallic region, we are also interested in the insulating region in order to examine the influence of pressure on CT gap insulator in general. On the other hand, the electrical conduction mechanism of $\text{La}_{2-x}\text{Sr}_x\text{NiO}_4$ is not clearly understood, although it has been studied by several groups.^{2,3,32-34} Previous measurements of midinfrared¹⁸ and x-ray³⁵ absorption in $\text{La}_{2-x}\text{Sr}_x\text{NiO}_4$ revealed the existence of small polarons. This will be examined herein through our pressure dependence of the electrical resistivity experiment in order to expand our understanding of the conduction mechanism of this system.

II. EXPERIMENTAL DETAILS

All $\text{La}_{2-x}\text{Sr}_x\text{NiO}_4$ samples were prepared from high purity La_2O_3 , SrCO_3 , and NiO which were oven dried prior to use. Stoichiometric quantities were thoroughly mixed, placed in dense Al_2O_3 crucibles, and calcined at 1150°C in air, followed by regrindings for 10 min; this step was repeated four times. Subsequently, the sample was reground and reacted at 1250°C for one day; this step was repeated three times. The undoped sample ($x=0$) was then pressed into pellets, reacted in argon at 1250°C for 16 h, and finally cooled to room temperature at a rate of $6^\circ\text{C}/\text{min}$. The remaining samples were reground and reacted in air at 1275°C for one additional day, reground, pressed into pellets, and reacted for 16 h at 1325°C for $x \leq 0.5$, 1350°C for $x = 0.6$ and 0.7 , and 1375°C for $x = 0.8-1.2$; these samples were all cooled in air to room temperature at $1^\circ\text{C}/\text{min}$. X-ray diffraction was used to check for impurity phases revealing a minor NiO impurity ($\leq 2\%$). Iodometric titration was used to determine the oxygen content δ ; the obtained δ values agree with those of Takeda² and Strangfeld *et al.*³³ For the chemical formula $\text{La}_{2-x}\text{Sr}_x\text{NiO}_{4+\delta}$, we found $\delta = -0.01 \pm 0.03$ for $0 \leq x \leq 0.8$. Samples with $x > 0.8$ exhibit a tendency toward oxygen deficiency ($\delta = -0.02 \pm 0.01$). The sample $\text{La}_2\text{NiO}_{4+\delta}$ was found to exhibit $\delta \sim 0.04 \pm 0.01$. All compositions remain chemically stable in air. The electrical resistivity as a function of temperature T ($4.2 \text{ K} \leq T \leq 300 \text{ K}$) was measured by a four-lead dc technique with pressure applied and maintained in a beryllium-copper self-clamping device using Fluorinert as the pressure transmitting fluid. All pressures are applied at room temperature in a hydrostatic fashion. Pressure was determined at room temperature with a calibrated manganin resistance gauge. Calibrated Pt- and Si-diode thermometers were used and all measurements were performed with cooling rates of about $0.5^\circ\text{C}/\text{min}$, in order to facilitate thermal equilibrium between the sample and thermometers.

III. ELECTRICAL RESISTIVITY AT AMBIENT PRESSURE

The electrical resistivity $\rho(T)$ of $\text{La}_{2-x}\text{Sr}_x\text{NiO}_4$ ($0 \leq x \leq 1.2$) is shown at ambient pressure in Fig. 1. The resistivities change by several orders of magnitude with x . For the compositions $0 \leq x \leq 0.5$, $\rho(T)$ grows quickly with decreasing temperature. The sudden increase in ρ below $T_{\text{CO}} = 260 \text{ K}$ for $x = 0.25$ is associated with charge ordering.⁵ For

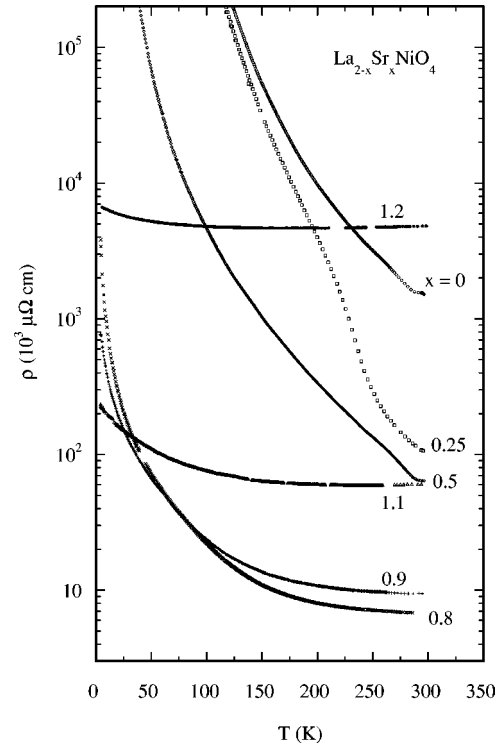


FIG. 1. Temperature-dependent resistivities ρ for various $\text{La}_{2-x}\text{Sr}_x\text{NiO}_4$ ($0 \leq x \leq 1.2$) compositions.

compositions $x \geq 0.9$ a metal-insulator ($M-I$) transition occurs whose transition temperature T_{MI} decreases monotonically with hole doping.² These are clearly seen from our data plotted in the inset of Fig. 2(b) and Fig. 10. Our resistivity data are in general agreement with those of Cava *et al.*,³ but our overall resistivities are larger and show a minimum around $x = 0.8$ instead of $x = 1.0$. The data of Takeda *et al.*² reveal a minimum in ρ below 300 K for $x = 1.2$. These differences likely arise from variations in oxygen stoichiometry and specimen densities.³

In order to examine the electrical conduction mechanism of $\text{La}_{2-x}\text{Sr}_x\text{NiO}_4$, $\rho(T)$ is compared to

$$\rho = \rho_0 \exp(E_g/k_B T), \quad (1)$$

which represents simple thermally activated electrical conductivity³⁶ in which an electron or hole (as the charge carrier) moves from one localized state to another due to an exchange of energy between the charge carrier and phonon (the localization is not a consequence of interaction with a phonon, but could occur due to a random electric field or disordered arrangement of atoms); in Eq. (1) ρ_0 is the electrical resistivity at extremely high temperatures, E_g is the thermal activation energy of the electron or hole, and k_B is the Boltzmann constant. Realizing that the specimens are polycrystalline, only general statements will be made here regarding the electrical conduction mechanism. The electrical resistivity of $\text{La}_{2-x}\text{Sr}_x\text{NiO}_4$ ($0 \leq x \leq 1.2$) is plotted as $\ln \rho$ versus $1/T$ in Figs. 2(a) and 2(b); since the data does not exhibit linear behavior through the entire temperature range, we conclude that Eq. (1) is an inadequate description. How-

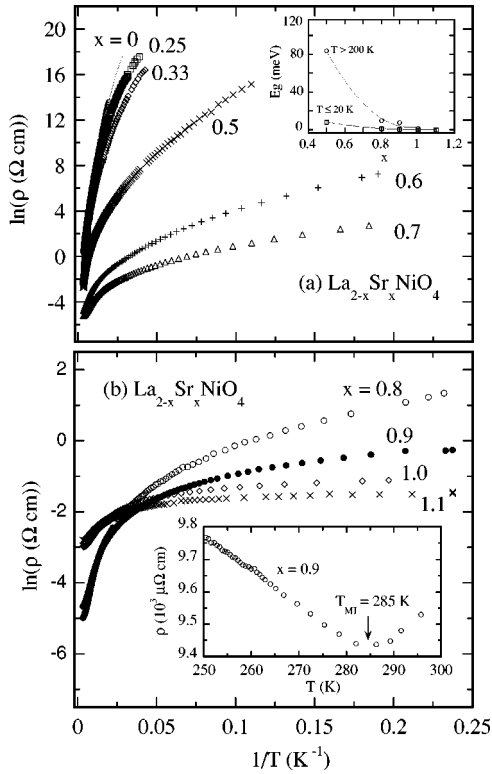


FIG. 2. Temperature-dependent resistivities for $\text{La}_{2-x}\text{Sr}_x\text{NiO}_4$ plotted as $\ln[\rho(\Omega \text{ cm})]$ vs $1/T (\text{K}^{-1})$. (a) $x < 0.8$; (b) $x \geq 0.8$. The insets of (a) show the value of E_g versus doping level x , and (b) exhibit the doping induced metal-insulator transition for $x = 0.9$.

ever, this equation can provide a rough idea of thermal activation energies in narrow temperature regions where the data can be fitted. In the range $200 \text{ K} \leq T \leq 260 \text{ K}$ (note that $T_{MI} \leq 285 \text{ K}$) the fits yield values of $E_g = 98 \text{ meV}$ for $x = 0$, 86 meV for $x = 0.5$, 10 meV for $x = 0.8$, and 8 meV for $x = 0.9$. Measurements on a single crystal with $x = 0.25$ shows a comparable value of $E_g = 105 \text{ meV}$ for ρ_a and ρ_c in this temperature range;³⁷ this suggests that our polycrystalline samples provide activation energies similar to those of single crystal samples. We note that the extracted activation energies are far smaller than the La_2NiO_4 CT gap of 3.5 eV (Refs. 38,39) formed between the Ni-3d and O-2p bands, this band gap differs from the Mott-Hubbard gap arising through splitting of metal Ni-3d bands. For compositions $x \geq 0.9$, above T_{MI} $d\rho/dT$ is positive indicating a charge carrier energy positioned in the conduction band; below T_{MI} ρ is thermally activated but with a value of E_g significantly smaller than that observed for compositions $x < 0.9$. In fact, E_g is substantially smaller for all compositions below 20 K as shown in the inset of Fig. 2(b) indicating a change in regime occurs in ρ for $20 \text{ K} < T < 200 \text{ K}$. The small charge carrier mobility of $\text{La}_{2-x}\text{Sr}_x\text{NiO}_4$, as seen in Fig. 1, is consistent with localization due to strong electron-phonon coupling^{5,17,40,41} which could be associated with polaronic conduction.^{24,36,37,42} Given the occurrence of charge ordering in this system, polaronic conduction seems a natural possibility. According to the Emin-Holstein theory,⁴² thermal-activated small polaron hopping leads to ρ in the form of

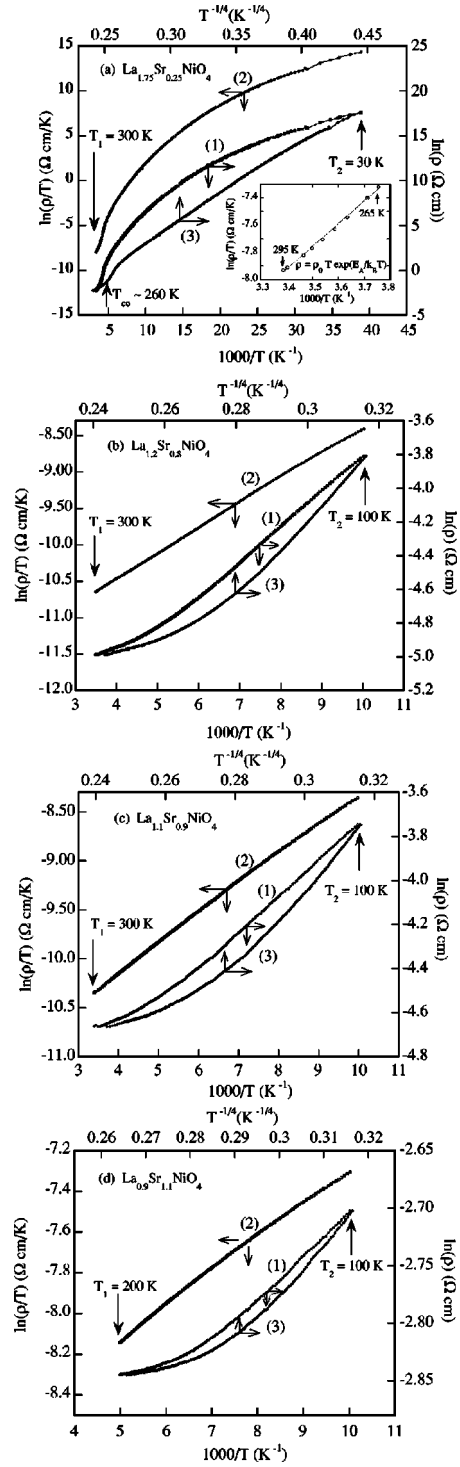


FIG. 3. Temperature-dependent resistivities for $\text{La}_{2-x}\text{Sr}_x\text{NiO}_4$ scaled for direct charge excitations above the mobility edge into the conduction band or thermally activated nearest-neighbor hopping of charges [curve (1), bottom + right axes], small polaron hopping [curve (2), bottom + left axes], and variable range hopping (VRH) [curve (3), top + right axes], over a wide range of temperature. (a) $x = 0.25$, (b) $x = 0.8$, (c) $x = 0.9$, and (d) $x = 1.1$. The perpendicular arrows on each curve specify the plot axes. The scaling models are as following: (1) $\rho = \rho_0 \exp(E_g/k_B T)$, (2) $\rho = \rho_0 T \exp(E_A/k_B T)$, and (3) $\rho = \rho_0 \exp(U/T^{1/4})$. The inset of (a) displays thermally activated polaron conduction [Eq. (2)] above T_{CO} for $x = 0.25$.

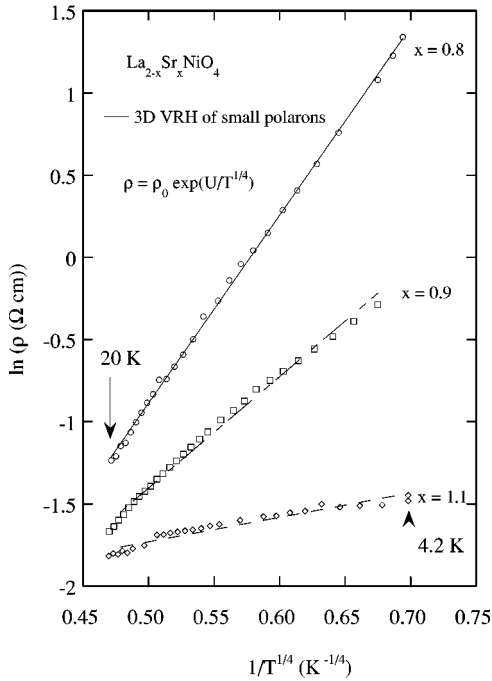


FIG. 4. Low temperature ($T < 20$ K) resistivities for $\text{La}_{2-x}\text{Sr}_x\text{NiO}_4$ ($x > 0.5$) show VRH behavior of small polarons.

$$\rho = \rho_0 T^\alpha \exp(E_A/k_B T), \quad (2)$$

where ρ_0 is a constant related to the polaron concentration and diffusion, E_A is the polaron hopping energy, and $\alpha = 1$ corresponds to the adiabatic case (in the nonadiabatic case, $\alpha = 1.5$). At low temperatures the polarons can still conduct despite the small available phonon energy. In this regime, three-dimensional variable range hopping (VRH) applies³⁶ with a temperature-dependent ρ given by

$$\rho = \rho_0 \exp(U/T^\beta), \quad (3)$$

where $\beta = 1/4$. In Eq. (3) ρ_0 and U are fitting parameters, U relates to the density of states $g(E_F)$ at the Fermi level E_F , i.e., $U \propto [g(E_F)]^{-1/4}$. For highly correlated electron systems, a small gap appears at E_F and $\beta = 1/2$.²⁹

Data in Fig. 3 are plotted in a manner which compares the various conduction mechanisms described by Eqs. (1)–(3). It is clear in Figs. 3(a)–3(d) that Eq. (1) does not provide the best fit over a wide temperature range in any case. For compositions $0 \leq x \leq 0.5$, T_{CO} has been attributed to the onset of polaron ordering;⁴ at some compositions, below T_{CO} hole-rich domain walls separate hole-poor AFM domains. This is a potentially ideal physical system whereby polaronic conduction should be observed at high temperatures where the charge carriers are fairly mobile, but dressed by the surrounding ions. At low temperature, two different nickel ionic species are frozen into discrete positions and the AFM ordered regions will likely be energy costly in hopping processes. Thus, any conducting holes will prefer to hop among nearest neighbors with similar energies, these will likely be the domain-wall regions; this scenario may best be described by VRH. In fact, we have found that at $T < T_{CO}$ for $x = 0.25$, Eq. (3) with $\beta = 1/4$, provides the best fit to our data

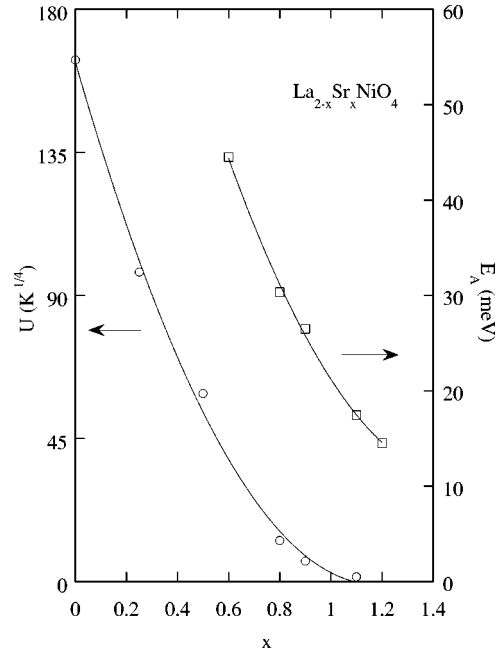


FIG. 5. Variation of small polaron conduction parameters E_A and U vs doping level x .

[see Fig. 3(a), for example]. The same behavior is true for $x = 0.33$ and 0.50 . Above T_{CO} , Eq. (2) applies, indicating that the contribution to the conductivity comes from the thermal activated hopping of small polarons. This can be seen by viewing Fig. 3(a) and its inset which illustrates fits above and below T_{CO} for $x = 0.25$ using Eqs. (2) and (3), respectively. For $x = 0$, the resistivity follows the 3D VRH Eq.(3) in the whole temperature range from 300 down to 30 K, but with $\beta = 1/2$ indicating a highly correlated electron system; measurements below 30 K were not possible with our apparatus.

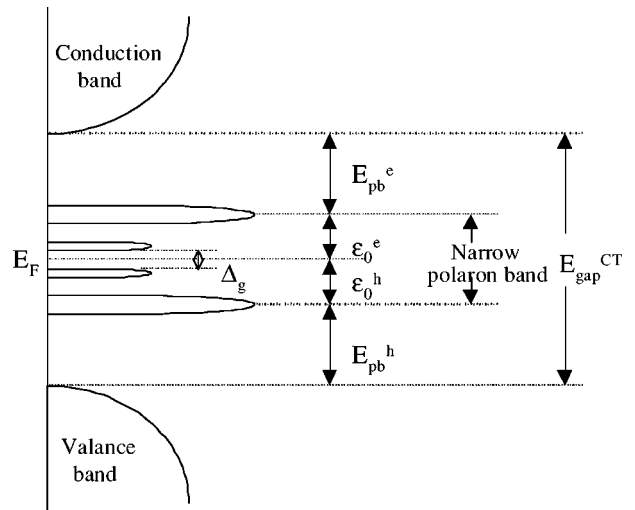


FIG. 6. A band diagram for e -ph coupled $\text{La}_{2-x}\text{Sr}_x\text{NiO}_4$ system with intrinsic charge carrier generations. $E_{\text{gap}}^{\text{CT}}$ is the charge transfer (CT) gap, E_{pb} is the polaron binding energy, ϵ_0 is the energy required to generate intrinsic charge carriers (e : electron, and h : hole) and Δ_g is a small gap at the Fermi level specifying high electron correlations in this system.

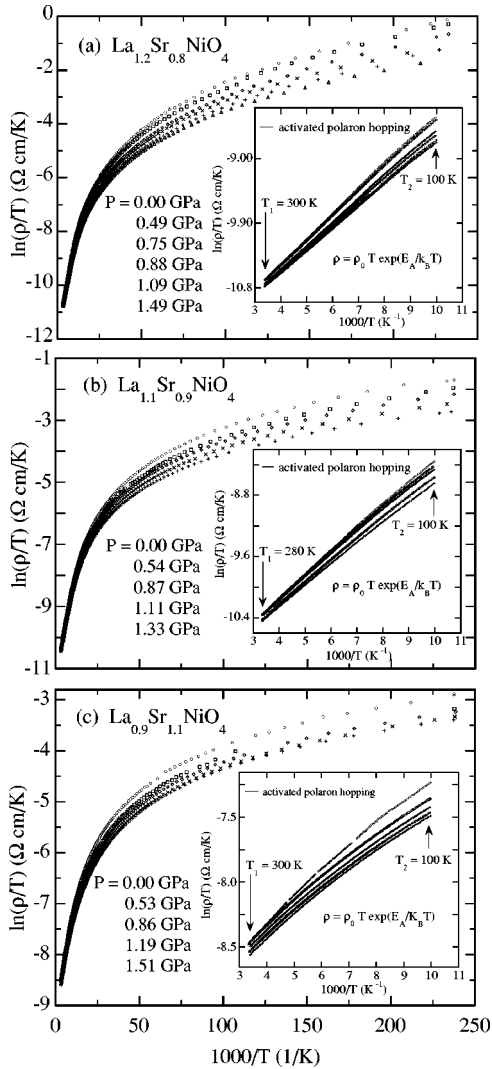


FIG. 7. The pressure effect on small polaron conduction from the measurement of the electrical resistivity ρ vs temperature for $\text{La}_{2-x}\text{Sr}_x\text{NiO}_4$ ($x \geq 0.8$) at the indicated pressures. The inset shows the pressure effect on the small polaron conduction from 100 K up to 300 K. (a) $x=0.8$, (b) $x=0.9$, and (c) $x=1.1$.

For compositions $x > 0.5$, Eq. (2) gives the best fit down to 100 K below T_{MI} [see Fig. 3(b), for example]. At low temperature ($T \leq 20$ K), Eq. (3) with $\beta = 1/4$ applies, as seen from Fig. 4. The same behavior is illustrated by the $x=0.9$ and 1.1 specimens as illustrated in Figs. 3(c) and 3(d) and Fig. 4. These observations suggest that at low temperatures the conduction is through VRH of small polarons that are bound to the holes (bound polarons) and at higher temperatures the conduction is dominated by thermal activation of the polarons. At the temperature above T_{MI} where $d\rho/dT > 0$ the electrical conduction comes from phonon scattering of polarons (free polarons) transporting as free heavy particles, according to the Emin-Holstein theory. This general picture is found to apply to all compositions of $\text{La}_{2-x}\text{Sr}_x\text{NiO}_4$ according to our data. This small polaron conduction mechanism in $\text{La}_{2-x}\text{Sr}_x\text{NiO}_4$ is also supported by thermopower³³ and Hall effect² measurements.

Figure 5 shows the fitted parameters U and E_A versus hole

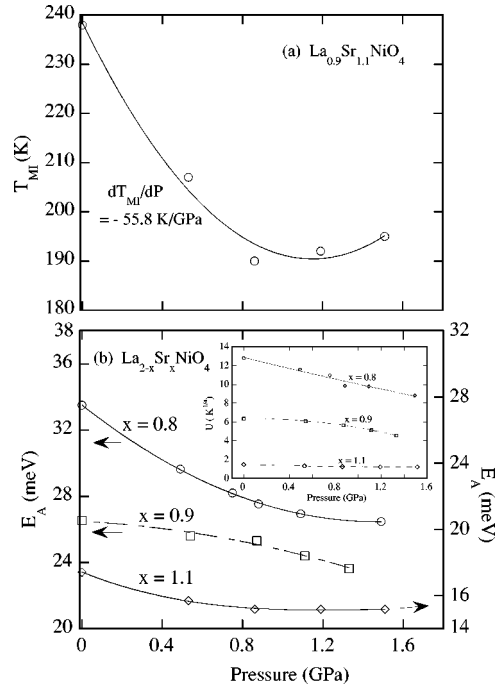


FIG. 8. (a) An example of pressure dependence of the metal-insulation transition temperature T_{MI} for $\text{La}_{2-x}\text{Sr}_x\text{NiO}_4$. (b) Pressure dependence of the small polaron conduction parameters E_A and U (the inset) for $\text{La}_{2-x}\text{Sr}_x\text{NiO}_4$.

doping x . Apparently U decreases with increasing x , indicating that the density of localized states at the Fermi level increases with Sr concentration. A systematic representation of the band diagram in this e -ph coupled system is presented in Fig. 6.

A narrow polaron band is formed because of the existence of a number of energetically equivalent sites in the crystal lattice. The Fermi energy resides in the polaron band and has a small gap Δ_g appearing at E_F because of high electron correlations²⁹ existing in the system. E_A also decreases with the increase of x , but with a smaller rate than U . Since E_A is associated with the activation energy ε_0 of the intrinsic charge carrier and the binding energy E_{pb} of a polaron and the electron transfer integral J between nearest neighbor sites, it is given by^{43,44}

$$E_A = \varepsilon_0 + E_{pb}/2 - J. \quad (4)$$

The parameter J is related to the polaron binding energy by the relation $J < E_{pb}/2$; a reasonable value^{18,44} is $J \sim E_{pb}/3$. The binding energy E_{pb} is related to the polaron size (radius r_p). These energy scales also relate to the CT gap E_{gap}^{CT} through the equation

$$E_{gap}^{CT} = 2E_{pb} + 2\varepsilon_0 \approx 2E_{pb}. \quad (5)$$

The parameter ε_0 can be determined from the thermopower S since the intrinsic charge carrier only involves entropy when it is thermally activated, thus $\varepsilon_0 \ll E_A$.⁴³ For example, with such measurements Strangfeld *et al.*³³ has shown that $d\varepsilon_0/dx < 0$ for $x > 0.5$ and $\varepsilon_0 \approx 7$ meV at $x=0.6$. Since we observe $dE_A/dx < 0$, we can see $dE_{pb}/dx < 0$, thus

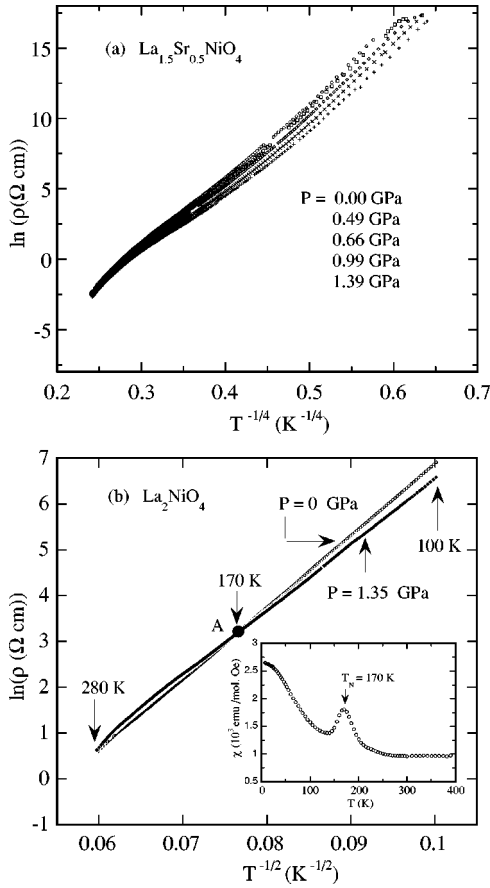


FIG. 9. The pressure effect on small polaron conduction from the measurement of the electrical resistivity ρ vs temperature for $\text{La}_{2-x}\text{Sr}_x\text{NiO}_4$ ($x \leq 0.5$) at the indicated pressures. (a) $x=0.5$. (b) $x=0$ (The inset is the temperature dependence of the magnetic susceptibility χ of La_2NiO_4).

$dE_{\text{gap}}^{\text{CT}}/dx < 0$. This aids in understanding the role of doping which decreases the CT gap thereby improving charge transport conductivity.

IV. ELECTRICAL RESISTIVITY UNDER PRESSURE

In Fig. 7, the pressure dependence of ρ plotted as $\ln(\rho/T)$ versus $1/T$ for representative $\text{La}_{2-x}\text{Sr}_x\text{NiO}_4$ ($x=0.8, 0.9$, and 1.1) specimens is displayed at five to six pressures in the range $0 \leq P \leq 1.6$ GPa. Pressure is observed to weakly decrease ρ . Near room temperature, a rate of $-8.2\%/GPa$ ($d\rho/dP \approx -0.57$ m Ω cm/GPa) is observed for $x=0.8$. Similar values of $-8.3\%/GPa$ ($d\rho/dP \approx -0.80$ m Ω cm/GPa) and $-6.9\%/GPa$ ($d\rho/dP \approx -4.81$ m Ω cm/GPa) are observed for $x=0.9$ and $x=1.1$, respectively.

Fits to the data in the temperature range from 100 up to 300 K provide the pressure dependence of the thermally activated polaron hopping energy E_A which is displayed in Fig. 8(b). We also find that T_{MI} is affected by pressure. For example, pressure drives T_{MI} for $x=1.1$, from ~ 238 K at $P=0$ GPa to ~ 190 K at 0.86 GPa providing a very large derivative of $dT_{MI}/dP \approx -55.8$ K/GPa as illustrated in Fig. 8(a). Pressures higher than ~ 1.0 GPa are observed to drive

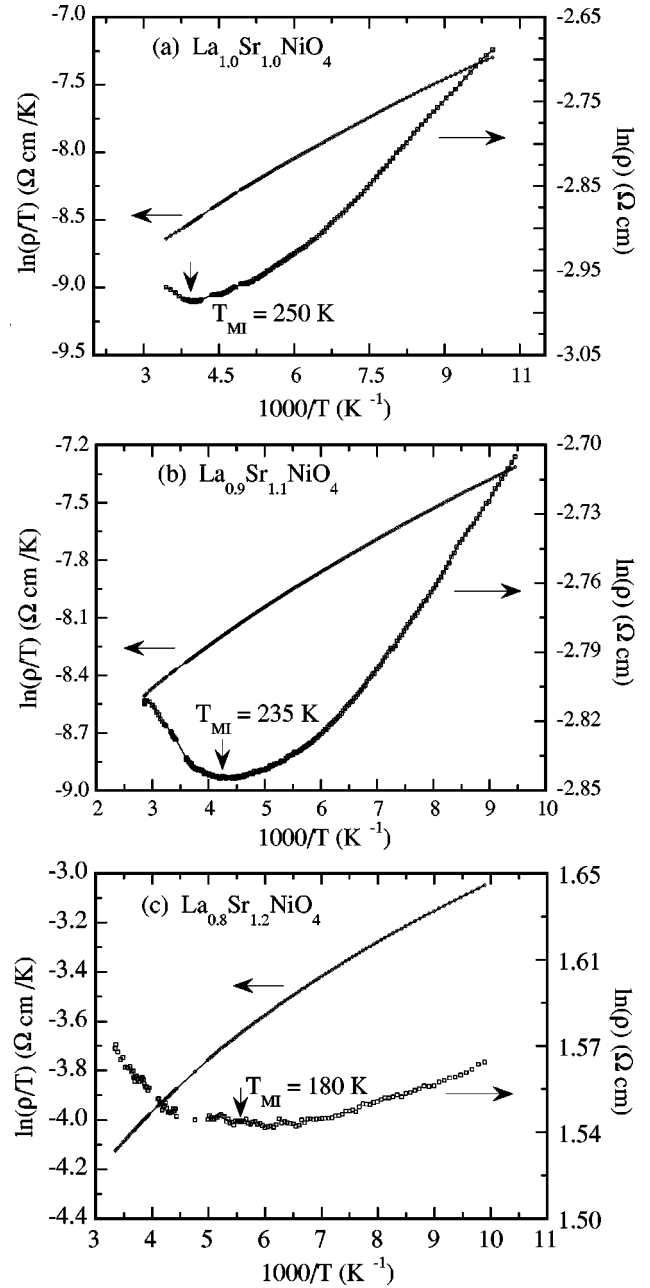


FIG. 10. Temperature-dependent resistivities plotted with appropriate abscissa to compare small polaron and semiconductor models across the T_{MI} region for $\text{La}_{2-x}\text{Sr}_x\text{NiO}_4$.

T_{MI} to slightly higher temperatures. At temperatures below 20 K, fits to the data plotted as $\ln(\rho)$ vs $1/T^{1/4}$ reveal the pressure dependence of the fitting parameter U which is displayed in the inset of Fig. 8(b).

Figure 9 shows the pressure dependence of ρ for $x=0$ and $x=0.5$. As we described in the previous section, the best fit for $x=0.5$ comes from the VRH conduction of small polarons with $\rho \sim \exp(U/T^{1/4})$ for $4.2 \text{ K} \leq T \leq 300 \text{ K}$ and for $x=0$ with $\rho \sim \exp(U/T^{1/2})$ for $30 \text{ K} \leq T \leq 300 \text{ K}$. For $x=0.5$, near 300 K, pressure decreases ρ at a rate of $-31.6\%/GPa$ ($d\rho/dP \approx -31.91$ m Ω cm/GPa) and at $P=0$ GPa the parameter $U \approx 59.1 \text{ K}^{1/4}$ and dU/dP

≈ -2.99 (K^{1/4}/GPa). Interestingly, all the pressure curves measured for $x=0$ cross at the same temperature $T_A = 170$ K. Above T_A pressure is observed to slightly increase ρ and below T_A pressure slightly decreases ρ [for clarity, only two pressure curves are shown in Fig. 9(b)].

In order to gather information that may be connected with this observation, we conducted magnetic susceptibility χ measurements; these data are plotted in the inset of Fig. 9(b). We found that 170 K is the temperature where a peak in χ occurs resulting from short range local AFM order associated with a possible onset of a low temperature orthorhombic (LTO) to tetragonal (LTT) transition, since this LTO to LTT transition ($Bmab$ to $P4_2/ncm$) usually happens at a temperature below the $M-I$ transition⁴⁵⁻⁴⁸ in $\text{La}_2\text{NiO}_{4+\delta}$. The fitted parameter U for $x=0$ at $P=0$ exhibits $U \approx 155.8$ K^{1/2} and $dU/dP \approx -9.98$ K^{1/2}/GPa. Since the resistivity reveals a very small pressure dependence both above and below T_A , this suggests that applied pressure does not appreciably change the localized states which exist at low temperature.

V. DISCUSSION

It is interesting that above T_{MI} for compositions $x \geq 0.9$ the resistivity of the polaron scattering process also behaves as $\rho \sim T \exp(E_A/k_B T)$, as revealed in Fig. 10. A change in slope is only noticeable in the $\ln(\rho)$ vs $1/T$ plot, but not in the $\ln(\rho/T)$ vs $1/T$ plot. This is also the indication of small polaron conduction.⁴⁹ On the other hand, from $\rho \sim T \exp(E_A/k_B T)$, we have

$$d\rho/dT = \exp(E_A/k_B T)(1 - E_A/k_B T). \quad (6)$$

At T_{MI} , $d\rho/dT=0$ and we see $E_A \equiv k_B T_{MI}$. Thus, T_{MI} is a direct measurement of the small polaron hopping energy E_A . Through Eqs. (4) and (5) it can be seen that this further reflects pressure-induced changes of the CT gap. With T_{MI} and E_A closely related, the pressure dependence of these parameters (illustrated in Fig. 8) can be reassessed. The pressure dependence of E_A appears small, but it in fact reflects a very large change in T_{MI} illustrating the strong effect which pressure has on the transition region from nonlocalized to localized polarons.

According to the Emin-Holstein theory,⁴² the polarons are quasiparticles (charge carriers) formed through electron (or

hole) polarization due to strong electron-phonon interaction. Above T_{MI} ($\sim \Theta_D/2$, where Θ_D is the Debye temperature), the polaron motion is that of delocalized heavy-particle carriers scattered by phonons, so the resistivity decreases with decreasing temperature [$d\rho/dT > 0$, see Eq. (6)]. Below T_{MI} ($d\rho/dT < 0$) the polarons are bounded to the impurity centers moving by phonon assisted hopping. At low temperatures $T < \Theta_D/4$, the motion of the charge carriers between equivalent sites is not thermally activated and the VRH of small polarons dominates the conduction. We are aware that $\Theta_D = 313$ and 331 K for $x=0.25$ and 0.33, respectively;⁵⁰ values at other compositions are unknown to us. For $x=0.25$ [see Fig. 3(a)], below approximately $\Theta_D/2$ we see VRH behavior, in contrast to the $\Theta_D/4$ prediction of Emin-Holstein theory, and that the temperature range over which Eq. (2) is valid appears to be T close to Θ_D and above. The similar temperature range is true for $x=0.33$ (not shown), but with a broader charge ordering transition area than $x=0.25$.

In conclusion, we have presented experimental results of pressure effect on the electrical resistivity of $\text{La}_{2-x}\text{Sr}_x\text{NiO}_4$ for the first time over a wide range of hole doping level x ($0 \leq x \leq 1.2$). We have shown strong direct evidence for small polaron transport in this $\text{La}_{2-x}\text{Sr}_x\text{NiO}_4$ system. The polaron conduction parameters E_A and U are functions of both hole doping level x and pressure P . The change of these parameters directly reflects the change of the density of states near the Fermi level and the CT gap. We have observed the compositionally induced $M-I$ transition below room temperature for $x \geq 0.9$ and T_{MI} decreases monotonically with the increase of doping. But pressure is shown to weakly affect the resistivity and T_{MI} cannot be completely suppressed, which implies that the applied pressure does not appreciably change the localized states at the Fermi level, and applied pressure alone cannot destroy the $M-I$ transition and the CT gap. No superconductivity was observed at pressures up to 1.6 GPa and temperatures down to 4.2 K.

ACKNOWLEDGMENTS

G. Wu would like to thank J. Cohn for the help of some low current measurement, and also acknowledge discussions with J. Leao, H. Terashita, and E. Timmins. This work is supported by National Science Foundation CAREER Grant No. DMR 9982834.

*Permanent address: Department of Physics and Astronomy, UCLA, Los Angeles, CA 90095.

†Permanent address: Department of Physics, Montana State University, Bozeman, MT 59717.

¹J. Gopalkrishnan, G. Colsmann, and B. Reter, *J. Solid State Chem.* **22**, 145 (1977).

²Y. Takeda, R. Kanno, M. Sakano, O. Yamamoto, M. Takano, Y. Bando, H. Akinaga, K. Takita, and J. B. Goodenough, *Mater. Res. Bull.* **25**, 293 (1990).

³R. J. Cava, B. Batlogg, T. T. Palstra, J. J. Krajewski, W. F. Peck, Jr., A. P. Ramirez, and L. W. Rupp, Jr., *Phys. Rev. B* **43**, 1229 (1991).

⁴C. H. Chen, S-W. Cheong, and A. S. Cooper, *Phys. Rev. Lett.* **71**, 2461 (1993).

⁵S. W. Cheong, H. Y. Hwang, C. H. Chen, B. Batlogg, L. W. Rupp, and S. A. Carter, *Phys. Rev. B* **49**, 7088 (1994).

⁶Z. Kakol, J. Spalek, and J. M. Honig, *Solid State Commun.* **71**, 283 (1989).

⁷J. Spalek, Z. Kakol, and J. M. Honig, *Solid State Commun.* **71**, 5114 (1989).

⁸S. A. Hoffman, C. Venkatraman, S. N. Ehrlich, S. M. Durbin, and G. L. Liedl, *Phys. Rev. B* **43**, 7852 (1991).

⁹J. M. Tranquada, D. J. Buttrey, and V. Sachan, *Phys. Rev. B* **54**, 12 318 (1996).

- ¹⁰V. Sachan, D. J. Buttrey, J. M. Tranquada, J. E. Lorenzo, and G. Shirane, *Phys. Rev. B* **51**, 12 742 (1995).
- ¹¹S.-H. Lee and S. W. Cheong, *Phys. Rev. Lett.* **79**, 2514 (1997).
- ¹²H. Yoshizawa, T. Kakeshita, R. Kajimoto, T. Tanabe, T. Katsufuji, and Y. Tokura, *Phys. Rev. B* **61**, R854 (2000).
- ¹³J. M. Tranquada, D. J. Buttrey, and D. E. Rice, *Phys. Rev. Lett.* **70**, 445 (1993); J. M. Tranquada, Y. Kong, J. E. Lorenzo, D. J. Buttrey, D. E. Rice, and V. Sachan, *Phys. Rev. B* **50**, 6340 (1994).
- ¹⁴P. Wochner, J. M. Tranquada, D. J. Buttrey, and V. Sachan, *Phys. Rev. B* **57**, 1066 (1998).
- ¹⁵J. M. Tranquada, P. Wochner, A. R. Moodenbaugh, and D. J. Buttrey, *Phys. Rev. B* **55**, R6113 (1997).
- ¹⁶T. Ido, K. Magoshi, H. Eisaki, and S. Uchida, *Phys. Rev. B* **44**, 12 094 (1991).
- ¹⁷V. I. Anisimov, M. A. Korotin, J. Zaanen, and O. K. Andersen, *Phys. Rev. Lett.* **68**, 345 (1992).
- ¹⁸X.-X. Bi, P. C. Eklund, and J. M. Honig, *Phys. Rev. B* **48**, 3470 (1993).
- ¹⁹S. A. Kivelson and V. I. Emery, *Strongly Correlated Electronic Materials: The Los Alamos Symposium 1993*, edited by K. S. Bedell (Addison-Wesley, Reading, MA, 1994).
- ²⁰J. B. Torrance, P. Lacorre, C. Asavaroenghi, and R. M. Metzger, *Physica C* **182**, 351 (1991); J. Zaanen, G. A. Sawatzky, and J. W. Allen, *Phys. Rev. Lett.* **55**, 418 (1985).
- ²¹X. Obradors, L. M. Paulius, M. B. Maple, J. B. Torrance, A. I. Nazzari, J. Fontcuberta, and X. Granados, *Phys. Rev. B* **47**, R12 353 (1993).
- ²²P. C. Canfield, J. D. Thompson, S.-W. Cheong, and L. W. Rupp, *Phys. Rev. B* **47**, R12 357 (1993).
- ²³J. J. Neumeier, M. F. Hundley, J. D. Thompson, and R. H. Heffner, *Phys. Rev. B* **52**, R7006 (1995).
- ²⁴Guoqing Wu, J. J. Neumeier, and M. F. Hundley, *Phys. Rev. B* **63**, R245120 (2001).
- ²⁵V. V. Struzhkin, R. J. Hemley, H. K. Mao, and Y. A. Timofeev, *Nature (London)* **390**, 382 (1997).
- ²⁶K. Shimizu, K. Suhara, M. I. Eremets, and K. Amaya, *Nature (London)* **393**, 767 (1998).
- ²⁷S. H. Han, M. B. Maple, Z. Fisk, S.-W. Cheong, A. S. Cooper, O. Chmaissem, J. D. Sullivan, and M. Marezio, *Phys. Rev. B* **52**, 1347 (1995).
- ²⁸S. A. Carter, T. F. Rosenbaum, P. Metcalf, J. M. Honig, and J. Spalek, *Phys. Rev. B* **48**, 16 841 (1995).
- ²⁹B. I. Shklovskii, and A. L. Efros, *Electronic Properties of Doped Semiconductors* (Springer, Berlin, 1984).
- ³⁰R. J. Cava, *Physica C* **282**, 27 (1997).
- ³¹Y. Kitaoka, K. Ishida, T. Kobayashi, K. Amaya, and K. Asayama, *Physica C* **153-155**, 733 (1988).
- ³²C. N. R. Rao, P. Ganguly, K. K. Singh, and R. A. Mohan Ram, *J. Solid State Chem.* **72**, 14 (1988).
- ³³Th. Strangfeld, K. Westerholt, and H. Beach, *Physica C* **183**, 1 (1991).
- ³⁴K. Sreedhar and J. M. Honig, *J. Solid State Chem.* **72**, 147 (1994).
- ³⁵P. Kuiper, D. E. Rice, D. J. Buttrey, L. H. Tjeng, and C. T. Chen (unpublished).
- ³⁶N. F. Mott and E. A. Davis, *Electronic Processes in Non-crystalline Materials* (Oxford University Press), 1979.
- ³⁷J. J. Neumeier, Guoqing Wu, A. L. Cornelius, Yi-Kuo Yu, K. Andres, and K. J. McClellan (unpublished).
- ³⁸T. Ido, K. Magoshi, H. Eisaki, and S. Uchida, *Phys. Rev. B* **44**, 12094 (1991).
- ³⁹V. I. Anisimov, M. A. Korotin, J. Zaanen, and O. K. Andersen, *Phys. Rev. Lett.* **68**, 345 (1992).
- ⁴⁰J. Zaanen and P. B. Littlewood, *Phys. Rev. B* **50**, 7222 (1994).
- ⁴¹R. J. McQueeney, J. L. Sarrao, and R. Osborn, *Phys. Rev. B* **60**, 80 (1999).
- ⁴²D. Emin and T. Holstein, *Ann. Phys. (N.Y.)* **53**, 439 (1969).
- ⁴³M. Jaime, M. B. Salamon, K. Pettit, M. Rubinstein, R. E. Treece, J. S. Horowitz, and D. B. Chrisey, *Appl. Phys. Lett.* **68**, 1576 (1996).
- ⁴⁴I. G. Austin and N. F. Mott, *Adv. Phys.* **50**, 757 (2001).
- ⁴⁵J. Rodriguez-Carvajal, J. L. Martinez, J. Pannetier, and R. Saez-Puche, *Phys. Rev. B* **38**, 7148 (1988).
- ⁴⁶J. D. Jorgensen, B. Dabrowski, Shiyu Pei, D. R. Richards, and D. G. Hinks, *Phys. Rev. B* **40**, 2187 (1989).
- ⁴⁷G. H. Lander, P. J. Brown, J. Spalek, and J. M. Honig, *Phys. Rev. B* **40**, 4463 (1989).
- ⁴⁸Note, T_{MI} for $\text{La}_2\text{NiO}_{4+\delta}$ is ~ 700 K, and the LTO to LTT transition ($Bmab$ to $P4_2/nm$) happens at ~ 70 K for $\delta=0$ and varies with δ ($\delta < 0.07$). Mixed $Bmab$ and $Fmmm$ phases occur for $0.07 \leq \delta \leq 0.13$ from 300 to 10 K, while a single $Fmmm$ phase occurs when $\delta > 0.13$; see Refs. 45–47 for more detail.
- ⁴⁹J. B. Goodenough, in *Progress in Solid State Chemistry*, edited by H. Reiss (Pergamon, Oxford, 1971), Vol. 5, Chap. 4, pp. 145–400.
- ⁵⁰Guoqing Wu, J. J. Neumeier, C. D. Ling, and D. N. Argyriou, *Phys. Rev. B* **65**, 174113 (2002).